Available online at www.sciencedirect.com
ScienceDirect
ISA Transactions 46 (2007) 289–302
www.elsevier.com/locate/isatrans

Cooperative-feedback control

Leonardo Giovanini*

Industrial Control Centre, University of Strathclyde, Graham Hills Building, 50 George Street, Glasgow G1 1QE, United Kingdom

Received 23 February 2006; accepted 26 December 2006
Available online 21 May 2007

Abstract

In this work a control structure capable of handling controllability problems, which emerge from the presence of constraints, and improve the performance of the system by coordinating the use of several manipulated variables is introduced. In this scheme, the primary manipulated variable is used to handle the transient response while the auxiliary manipulated variable is used to keep the primary manipulated variable away from saturation. These two manipulated variables are coordinated through a user-defined non-linear function, which decides when and how the control structure changes. Its parameters determine the interaction between both inputs and the steady state value of each manipulated variable. The effectiveness of the proposed scheme is illustrated in two simulation examples.

Keywords: Input constraint; Multi-input systems; Habituating control

1. Introduction

In industrial control, PID technology is firmly established as *the standard*. Often, however, high control loop performance can only be obtained within narrow limits around a given steady-state operating point. If perturbations introduced by any reference or load change are outside these limitations then the actuators will constrain the system inputs. A typical method for dealing with input and output constraints, especially for PID control, has been the design and implementation of input and output conditioning techniques [1,2]. In research, anti-windup has become a recognized topic since 1980s [3–5] with many publications, research orientated books (e.g. [5,6]) and at scientific conferences.

When manipulated a variable is confined to a finite operating range anti-windup methods may work well under nominal conditions under which the controller was designed [5,7]. However, it is possible that under a large set-point change, a load disturbance or a component failure, the manipulated variable of the system will reach its limit while the system output still cannot reach its set-point at the steady state. This phenomenon is known as *output-unreachability under input constraint* [8], and it is directly associated with the size of the *operational space* of the system.

This problem is sometimes solved by modifying the control structure, but many times the process itself requires substantial changes. On the other hand, cooperative and habituating control schemes solve the output-unreachability problem by using a combination of inputs [8–12], and many times they introduce a degree of optimality in the solution [12]. Nevertheless, manipulated variable constraints are never completely eliminated because these techniques only solve the unreachability problem for steady-state. Therefore, there is a need of finding control structures able of broadening controlled operation spaces while preserving good performances and optimality.

In this work, a *control structure* capable of handling controllability problems, which emerge from the presence of constraints in the system inputs, by broadening the operation space through the combination and coordination of the several manipulated variables is developed. The structure can be summarized as two controllers connected through a specially designed non-linear function. This function decides, based on the value of the manipulated variable, when and how the control structure changes, and therefore it defines how the manipulated variables are employed. Its parameters control the interaction between both manipulated variables and their steady-state values. The paper is organized as follows:

* Tel.: +44 151 548 2666; fax: +44 151 552 2487.
E-mail address: l.giovanini@eee.strath.ac.uk.

0019-0578/$ - see front matter © 2007 Published by Elsevier Ltd on behalf of ISA.
doi:10.1016/j.isatra.2006.12.001

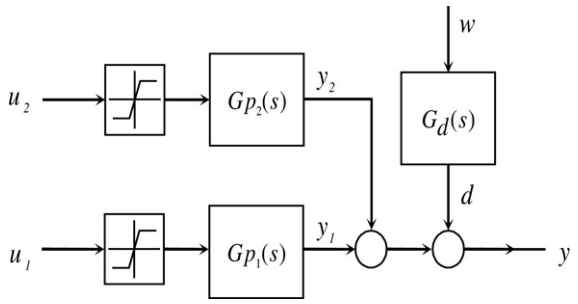

Fig. 1. Basic process structure.

the problem formulation and preliminaries are presented in Section 2. The cooperative-feedback control is proposed in Section 3. The structure of the Smith predictor is extended for the new control structure at the end of this section. In Section 4 two tuning procedures for the controllers are proposed. The first method is based on PID controllers and it is obtained from Internal Model Control (IMC) controller parametrization. The second procedure employs more sophisticated controllers. Some guidelines for the selection of the decision function parameters are also presented. Section 5, addresses the stability analysis of the resulting closed-loop. Finally, the results obtained from the application of the proposed algorithm to a linear system and a two heat-exchanger process are presented in Section 6 and conclusions are presented in Section 7.

2. Problem formulation and preliminaries

For simplicity, the discussion will be restricted to a multiple inputs–single output (MISO), however, the ideas presented in this work can be extended to MIMO systems. Fig. 1 shows a sketch of the process structure considered in this work, which is described by the transfer function models:

$$y(s) = Gp_1(s)u_1(s) + Gp_2(s)u_2(s) + G_d(s)w(s). \quad (1)$$

The first special feature to be noted is that the output variable y may be controlled by either u_1 or u_2 through different dynamic elements $Gp_1(s)$ and $Gp_2(s)$. The process may be also subject to many disturbances. For linear systems, they can be collectively represented by one disturbance d entering the process at the output. Along this paper, w is assumed to be a stochastic stationary or a deterministic signal. The dynamic element Gp_1 is faster and has a smaller time delay than Gp_2. A hard constraint might become active at some given extreme values of both manipulated variables.

In normal operation, the system is designed so that for any moderate set-point or load disturbance change, the manipulated variable u_1 can regulate the process output to achieve a zero output steady-state error working within its working range ($u_1 \in [u_{1\min}, u_{1\max}]$), while u_2 is kept unchanged. The input u_1 has a more direct effect (fastest dynamic) on the output y than input u_2, however it is more expensive than u_2. In a habituating control systems, the fast input u_1 can be used to track setpoints changes and reject disturbances rapidly. As the slower input u_2 begins to affect the output, the fast input can habituate by slowing returning to its desire value. Because the expensive fast input, u_1, is not used at steady state, improved performance can be obtained with little additional cost.

This problem is frequently found in practice, so it deserves special research. One example can be found in the temperature control of thermical integrated chemical process [13]. A simple configuration of this type of system is given by two heat exchangers in series (Fig. 2): one heat exchanger (I_1) and a service equipment (S). This arrangement is very common in practice when besides the task of reaching a final temperature target on a process stream (T_{h_1}) there is an extra goal like maximum energy recovery. The heat exchanger(s) I_1 (I_i) is specifically designed for recovering the exceeding energy in the process stream h_1, and the service equipment S completes the thermic conditioning through an utility stream s [14]. The heat exchanger operates at a constant flowrate that maximizes the energy recovering on nominal conditions and the service S is designed to cope with the long-term variations on the inlet streams (h_1, c_1, c_i) conditions or having the capability of changing stream temperature T_{h_1} targets. In the case of a disturbance or setpoint change, the steady state may deviate. There could exist a situation, in which the effect is so large that the temperature cannot return to the set-point even when the service hits its limits. In such case, the auxiliary manipulated variable u_2, i.e. the flowrate of the heat exchanger I_1, has to

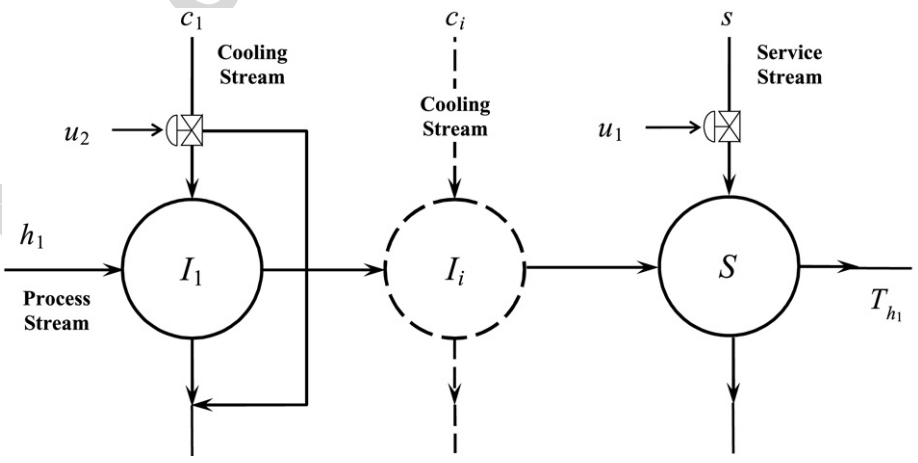

Fig. 2. Heat-exchanger process.

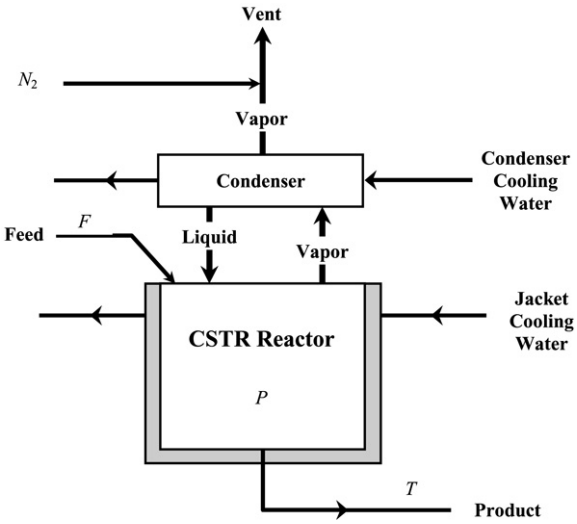

Fig. 3. Polymerization process.

be adjusted to make the temperature's steady state reach the desired value. In this example, the flowrate of the service $S(u_1)$ is the *expensive* manipulated variable because of the energy cost to produce the service. On the other hand, the flowrate of the heat exchanger $I_1(u_2)$ is the *cheap* manipulated variable because there is no cost to produce stream c_1.

Another example is a process for manufacturing certain acrylic resin consists of a continuous stirred tank polymerization reactor and an overhead cooling water exchanger [15], shown in Fig. 3. The feed to the reactor consists of monomer, initiator and solvent. The exchanger is used to condense solvent and monomer vapors, and a cooling water jacket is available to cool the reactor contents. The process also includes a vent line for condensables and a nitrogen admission line that can be used to control the reactor pressure P. One control objective is to control the reactor temperature T; the cooling water flowrate and the pressure (which can be changed almost instantaneously via nitrogen admission) are the principal manipulated variables. The reactor pressure has a much more rapid and direct effect on temperature than does the coolant flowrate. However, because significant and/or extended pressure fluctuations affect the reaction kinetics adversely, it is desirable to maintain the pressure near its setpoint. In this process, the coolant flowrate can be used as primary manipulated variable and the pressure as the secondary input. In this example, the nitrogen admission (N_2) is the *expensive* manipulated variable because of its adverse effects in the closed-loop performance (the change the reaction kinetics degrades the closed-loop performance due to uncertainty introduced in the loop), while the coolant flowrate is the *cheap* manipulated variable because it does not affect the reaction kinetics.

3. Cooperative control

The examples of output unreachability provided in the previous section are only few of many industrial cases. Such cases require changes in the value of the secondary manipulated variable and its coordination with the primary manipulated variable. The idea of solving the unreachability problem by using the secondary manipulated variable has been implemented in several control strategies during the past decades: these include valve position control [16]; coordinated control [17,18]; parallel control [19]; cooperative control [12,20] and flexible-structure control [21]. In general, with the exception flexible-structure control, these control strategies solve the unreachability problem only for steady-state without exploiting specific characteristics and operating objectives.

On the other hand, *habituating control techniques* [22,23] have been explicitly formulated to exploit the specific characteristics and operating objectives of the processes considered in this work. They coordinate how both manipulated variables are used, in order to solve the unreachability problem and optimize the system simultaneously. However, in case of actuator saturation or failure the closed-loop response is driven in an open-loop manner due to the fact that the setpoint for the auxiliary manipulated variable should be updated in open-loop way, and there are no parameters available to handle the balance between control quality and other process goals.

The control problem described in previous paragraphs requires an appropriated design that would be able to take advantage of the specific characteristics of the process, transfer the control from one manipulated variable to another and, if its possible, leaves the capability for handling the balance between performance and other goals to the operator. Hence, to solve this manipulated constraint problem requires a process engineering approach capable of combining control strategy and process efficiency. Because there are two manipulated inputs and one controlled output, the combination of control actions required to produced the desired output r_0 at steady-state is nonunique. Additional objectives are therefore required to obtain a well-defined control problem. In habituating control problems such as those described earlier, the fastest input (u_1) should also track a desired value (u_0) asymptotically while the other input is in the operating range ($u_2 \in [u_{2\min}, u_{2\max}]$). If the output-unreachability under input constraint phenomenon happens ($u_2 \notin [u_{2\min}, u_{2\max}]$), the system should be capable of maintain the controllability of the system. The desired control objectives are therefore as follows:

1. Obtain a desire transfer function between r and y;
2. Achieve asymptotic tracking of the setpoint (r) and auxiliary input (u_0) references despite plant/model mismatch;
3. Avoid the output-unreachability phenomenon;
4. Ensure nominal performance and robust closed-loop stability.

Note that if there is a controller C_1 handling u_1 to control y at a given setpoint value r_0, the stationary value expected for the controlled variable is $Gp_1(0)u_1(0)$, and if an integral mode is present, the manipulated variable goes to $u_1(0) = Gp_1^{-1}(0)r_0$. Let us assume now that just a fraction of this output y can be handled through the manipulated u_1 (this implies that a control constraint is active at a given level), and that an additional capacity can be provided through u_2. Then, there are two ways of defining the protection for regulation and operability:

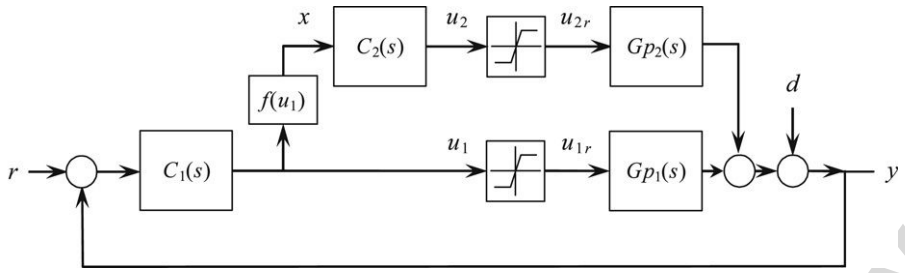

Fig. 4. Block diagram of reactive protection.

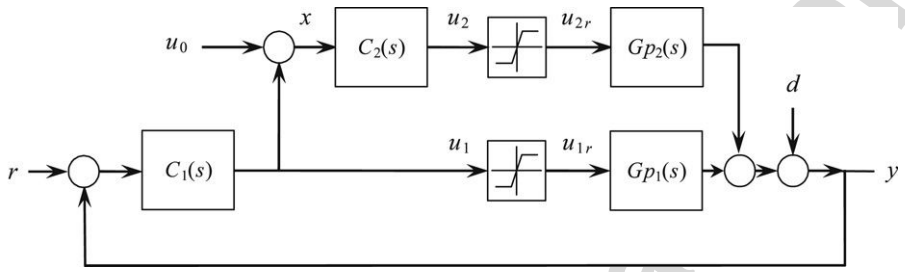

Fig. 5. Block diagram of cooperative action.

1. *Feedback or reactive protection*: given the instant manipulated variable u_1 at an operating point such that $u_1 \notin [u_{1\min}, u_{1\max}]$, $Gp_2(s)$ provides the complementary output ($Gp_1(0)\,[u_1(t) - u_{1\max}]$ or $Gp_1(0)\,[u_1(t) - u_{1\min}]$) in order to keep the system controllability.
2. *Cooperative action*: given a setpoint change r_0, Gp_2 should provide the output steady-state fraction $r_0 - Gp_1(0)u_0$ of the output y such that it reaches the target r_0 while $u_1(0) = u_0$.

These two operational modes are schematized in Figs. 4 and 5, where a second controller C_2 is included for better dynamic adjustment of the secondary manipulated variable u_2. They introduce a new feedback loop that results from combining both controllers, C_1 and C_2 in a single controller $C = C_1C_2$.

In the case of the reactive protection (Fig. 4), the output y is controlled by C_1 as long as the primary manipulated variable is not saturated, and the secondary control loop is not active because the auxiliary signal x is zero. When $u_1 \notin [u_{1\min}, u_{1\max}]$, the original control loop remains open and consequently inactive as long as u_1 is saturated. Then, the process part represented by Gp_2 is now in charge of the regulation. As soon as the structure of the system changes, due to the saturation of u_1, the structure of the controller is modified from C_1 to C following the change of the system and adapting the structure and parameters of the controller to the dynamic of the system. The controller C must include an anti-windup scheme to mitigate the effect of the constraint on u_2, the effect of constraint on u_1 is compensated by the control structure. The switching element is implemented through a simple nonlinear decision function such that the signal x entering the controller C_2 is given by:

$$f(u_1) = \begin{cases} u_1(t) - u_{1\max} & u_1(t) > u_{1\max}, \\ 0 & u_{1\min} \le u_1(t) \le u_{1\max}, \\ u_1(t) - u_{1\min} & u_{1\min} > u_1(t). \end{cases} \quad (2)$$

The switching function (2) can be easily implemented using a dead zone of width $u_{1\max} - u_{1\min}$ such that it generates the proper signal for each auxiliary loop. In general, given the characteristics of the system and the objectives of this control structure, the controller C_1 should include an integral model to ensure a free offset response (C_1 is at least a PI), while the controller C_2 is employed to speed up the response of the secondary loop (C_2 is at least a PD) [21]. In spite that a nonlinearity is introduced in the control loop, to transfer the control from Gp_1 to Gp_2, the stability properties of the system remain unaffected because there is no interaction between both control loops: when one manipulated variable is active the other is inactive.

In the case of the cooperative action (Fig. 5) the output y is controlled by both manipulated variable simultaneously (C_1 and C_2) but in different time scale. While the controller C_1 is used to regulate the plant, C_2 is used to get C_1 out of saturation. Usually C_1 has high bandwidth but will saturate for large error e. Controller C_2 attempts to control the plant to drive the output of controller C_1 to u_0. This has the effect of pushing the system back to the linear range of C_1's output. In general, the controller C_2 has a much lower bandwidth than C_1. The bandwidth separation makes it fairly easy to ensure the closed-loop stability.

Functions (2) represent the feedback protection exclusively, however a single structure can also be developed to include the cooperative action in the control loop. It is achieved by modifying the switching function (2) through the inclusion of the linear term:

$$\eta\,(u_1(t) - u_0) \quad \eta \ge 0, \forall u_1 \in [u_{1\min}, u_{1\max}]\,. \quad (3)$$

In general, given the characteristics of the system and the objectives of this control structure, the controllers C_1 and C_2 should include an integral model (C_1 is at least a PI while C_2 is at least a PID) to ensure that the variables y and u_1 track their

reference. The new term defines a permanent and increasing level of protection, when the control variable u_1 approaches the constraints, and the decision function (2) is now given by:

$$f(u_1) = \begin{cases} \widetilde{u}_1(t) + (\eta - 1)\widetilde{u}_{1\max} & \widetilde{u}_1(t) > \widetilde{u}_{1\max}, \\ \eta\widetilde{u}_1(t) & \widetilde{u}_{1\min} \le \widetilde{u}_1(t) \le \widetilde{u}_{1\max}, \\ \widetilde{u}_1(t) + (\eta - 1)\widetilde{u}_{1\min} & \widetilde{u}_{1\min} > \widetilde{u}_1(t), \end{cases} \quad (4)$$

where $\widetilde{\ }$ refers to the deviation of the variables to the parameter u_0:

$$\widetilde{u}_1(t) = u_1(t) - u_0, \qquad \widetilde{u}_{1\max}(t) = u_{1\max} - u_0,$$
$$\widetilde{u}_{1\min} = u_{1\min} - u_0. \quad (5)$$

If $\eta = 0$ the *split-range control* [16] is recovered, the decision function (4) becomes (2), and the auxiliary variable u_2 is used just to cover output demands when u_1 saturates only, which corresponds to the reactive protection. On the other case, when $\eta = 1$ the *Venier loop scheme* [22] is obtained. When $\eta > 0$ the auxiliary variable u_2 is used to prevent the saturation of u_1, driving the manipulated variable to u_0 by providing the fraction $r_0 - Gp_1(0)u_0$ of y while $u_2 \in [u_{2\min}, u_{2\max}]$. Both manipulated variables are simultaneously acting on the system, but with different gains: Kp_1 for u_1 and ηKp_2 for u_2, where $Kp_i = Gp_i(0)\, i = 1, 2$ is the gain of $Gp_i(s)$. This fact leads to interactions between both control loops that keeps the fastest loop working in the whole operational range maintaining a good control quality in the entire operational space without increasing the cost. When $u_1 \notin [u_{1\min}, u_{1\max}]$ the control system temporarily changes the structure and the portion of the process represented by Gp_2 controls the system output until Gp_1 becomes active again ($u_1 \in [u_{1\min}, u_{1\max}]$). In this control structure, u_2 is the first manipulated to saturate. When $u_2 \notin [u_{2\min}, u_{2\max}]$ the control system changes the structure permanently and only Gp_1 controls the system output.

Remark 1. The cooperative-feedback control keeps the fastest loop working all the time, because the steady-state is provided by the secondary manipulated variable, leading to a performance improvement with a minimum effect on the operational costs.

A second parameter can be included in the above formulation to start the cooperative action outside of the interval $[u_0 + \kappa, u_0 - \kappa]$, instead of doing it all the time. This new parameter introduces a region around the stationary value u_0 where only the fastest loop controls the system, and the decision function (4) is given by:

$$f(u_1) = \begin{cases} \widetilde{u}_1(t) + (\eta - 1)\widetilde{u}_{1\max} - \eta\kappa & \widetilde{u}_1(t) > \widetilde{u}_{1\max}, \\ \eta\,(\widetilde{u}_1(t) - \kappa) & \kappa < \widetilde{u}_1(t) \le \widetilde{u}_{1\max}, \\ 0 & -\kappa \le \widetilde{u}_1(t) \le \kappa, \\ \eta\,(\widetilde{u}_1(t) + \kappa) & \widetilde{u}_{1\min} \le \widetilde{u}_1(t) < -\kappa, \\ \widetilde{u}_1(t) + (\eta - 1)\widetilde{u}_{1\min} + \eta\kappa & \widetilde{u}_{1\min} > \widetilde{u}_1(t). \end{cases} \quad (6)$$

Fig. 6 shows a sketch of this function for different parameter values. Both parameters of the decision function, η and κ, can be used as tuning parameters to satisfy additional process' goals than control ones like process efficiency.

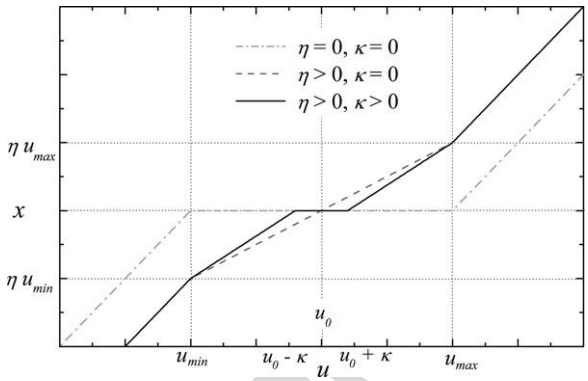

Fig. 6. Plot of the decision function for some values of the parameters η and κ.

Remark 2. Observe that for $\eta = 0$ the control action is executed over a *divided range*, that is: the second actuator starts moving once the first one saturates. This movement is temporal, because u_2 is used to restore the controllability of Gp_1. For positive values of η, the steady-state value of u_1 is driven to $u_0 \pm \kappa$. The magnitude of κ determine the region where only u_1 controls the system output, and indirectly defines the *common range*.

The capability of transferring the control from one input to another provides of implicit fault-tolerant capabilities to cooperative-feedback control. This fact means when a major fault in the actuator of u_2 happens, like a actuator frozen at a given a value, the cooperative-feedback structure is able to transfer the control of the system output to u_1, when $u_2 \notin [u_{2\min}, u_{2\max}]$, without any extra information than a measurement of the system output y. In case of a minor fault, like a loss a actuator sensibility, it can lead to output unreachability problem that is overcame as has been explained in the previous paragraph.

Time delay is a common feature in most of the process models. Control of systems with dominant time delay are notoriously difficult. It is also a topic on which there are many different opinions concerning of PID control. The response to command signals can be improved substantially by introducing *dead time compensation* [24]. The *dead time compensator*, or Smith predictor, is built by implementing a local loop around the controller with the difference between the model of the process without and with time delay.

Now, the structure of the Smith predictor is modified to consider the proposed control structure. In this case a second loop is introduced to represent the effect of u_2 over the system output. This fact leads to a new structure that include the models of both process ($\widetilde{G}p_1$ and $\widetilde{G}p_2$) and the constraints in the manipulated variables (see Fig. 7). The nonlinearities are required to follow the changes in the structure of the system. This structure works for time delays with different values as we can see in the examples. One can notice that a Smith predictor can be coupled with a robust controller (H_∞, *QFT*, robust pole placement, etc.) to cope with parametric variations.

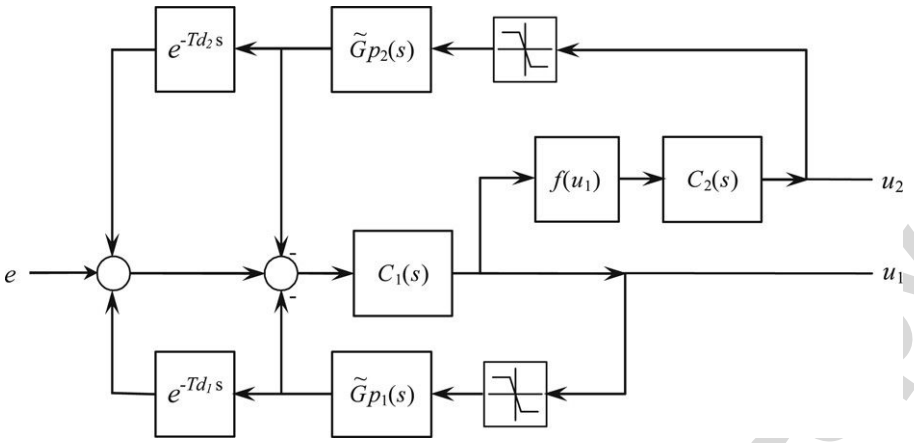

Fig. 7. Block diagram of Smith predictor for cooperative control.

4. Controller design and tuning

For designing and tuning the controllers involved in the cooperative-feedback structure it is necessary to analyse each control condition separately:

1. The first control structure is when controller C_1 is in charge of regulation of y, i.e. $u_1 \in [u_0 - \kappa, u_0 + \kappa]$ or $\eta = 0$.
2. The second control structure is defined by the secondary loop only, that is $u_1 \notin [u_{1\,\min}, u_{1\,\max}]$; the controller in this case is the combination $C = C_1 C_2$.
3. The third control condition appears when both loops are acting simultaneously, i.e. $\eta > 0$ and $u_1 \notin [u_0 - \kappa, u_0 + \kappa]$.

This decomposition of the problem indicates that the controller C_1 must be adjusted for high quality control when the process part Gp_1 handles the regulation, i.e. $u_1 \in [u_0 - \kappa, u_0 + \kappa]$; and this is essentially the traditional tuning problem for a single feedback loop. When $u_1 \notin [u_{1\,\min}, u_{1\,\max}]$, the process part Gp_2 must provide the complementary effect on the controlled variable, which means that controller C_2 must be combined with C_1 such to obtain the best possible performance.

In the following subsections two approaches for designing and tuning controllers C_1 and C_2 are presented. One is based on IMC parametrization of the controllers, the other is based on cancelation design criteria. In the IMC design the order of the process will be constrained to one and two, leading to PI and PID controllers. In the cancellation design, the constraint in the order of the systems is removed and the controllers can be designed by any controller design technique.

4.1. IMC design

For simplicity, let's assume stable plants, such that first or second order plus time delay models are adequate for describing the dynamics. Then, the IMC strategy provides a rapid parametrization of traditional PI or PID controllers [25]. If two PID algorithms with time delay compensation are proposed for controllers C_1 and C_2, recall that they work in series, i.e. the outlet of controller C_1 is the input to C_2 through the switching function $f(u_1)$. The following few hypothesis and practical reasons allow the selection of some important terms and the elimination of others:

- The double integration term is necessary since offset elimination is required for setpoint changes and disturbances.
- The control system structure assumes Gp_1 is faster and with smaller time delay than Gp_2, this could be a main argument for selecting u_1 as *primary* manipulated variable and u_2 as *secondary* manipulated.

These arguments support the selection – for instance – of controller C_1 as a PI controller:

$$C_1(s) = K_{C_1}\left(1 + \frac{1}{T_{I_1} s}\right), \tag{7}$$

and controller C_2 as a PID controller:

$$C_2(s) = K_{C_2}\left(1 + \frac{1}{T_{I_2} s} + T_{D_2} s\right). \tag{8}$$

These hypotheses lead to the following adjustment procedure:

1. Approximate the dynamics relating y and u_1 with a first-order plus time-delay transfer function

$$Gp_1(s) \cong Kp_1 \frac{\mathrm{e}^{-T_{d1} s}}{\tau_{p1} s + 1};$$

2. Use the IMC [26] parametrization to define the parameters of controller C_1, which is based on the Smith predictor structure, i.e.

$$K_{C_1} = 2\frac{\tau_{p1}}{Kp_1 \lambda_1}, \tag{9a}$$

$$T_{I_1} = \tau_{p1}; \tag{9b}$$

3. Approach the dynamics relating variables y and u_2 with a second-order plus time-delay model:

$$Gp_2(s) \cong Gp_1(s) Gp^*(s) = Kp_2 \frac{\mathrm{e}^{-T_{d2} s}}{(\tau_{p1} s + 1)(\tau_{p2} s + 1)} \tag{10}$$

where one of the time constant is arbitrarily made equal to τ_{p1}, the time constant determined for the model Gp_1. This condition is just a convenient way to get consistent individual and combined adjustments for controllers C_1 and C. Notice this still leaves three parameters, Kp_2, τ_{p2} and T_{d_2} to adjust the dynamic model Gp_2 to the correspondent physical data.

4. Follow the IMC parametrization procedure for the resulting model of the combination of controller C_1 and Gp_2

$$\widetilde{G}p(s) = C_1(s)Gp_2(s) = \frac{Kp_2}{Kp_1\lambda_1}\frac{\mathrm{e}^{-T_{d2}s}}{s\left(\tau_{p2}s+1\right)}$$

and a ramp reference signal. It gives a PID controller based on a Smith predictor structure. The parameters of the controller C_2, K_{C_2}, T_{I_2} and T_{D_2}; are given by the following relationships [26]

$$K_{C_2} = \frac{Kp_1\lambda_1}{Kp_2}\frac{2\lambda_2+\tau_{p2}}{\lambda_2^2}, \tag{11a}$$

$$T_{I_2} = 2\lambda_2 + \tau_{p2}, \tag{11b}$$

$$T_{D_2} = \frac{2\lambda_2\tau_{p2}}{2\lambda_2+\tau_{p2}}. \tag{11c}$$

Note that the procedure leaves two parameters, λ_1 and λ_2, for adjusting both controllers to achieve robust performance of the closed-loop system. Under the presence of uncertainties the system output y is given by:

$$y(s) = \left\{\widetilde{G}p_1(s)\left[1+lm_1(s)\right] + C_2(s)\widetilde{G}p_2(s)\left[1+lm_2(s)\right]\right\}u_1(s), \tag{12}$$

where $\widetilde{G}p_1$ and $\widetilde{G}p_2$ are the nominal models, lm_1 and lm_2 are the multiplicative uncertainties. Using the approximation (10) for $\widetilde{G}p_2$ and the tuned procedure proposed in this section for C_2, based on the IMC design procedure:

$$C_2(s) = \left\{\widetilde{G}p^*(s)\right\}_+^{-1} f_2(s), \tag{13}$$

where the filter $f_2(s)$ is given by [25]

$$f_2(s) = \frac{2\lambda_2 s+1}{\lambda_2 s}.$$

Then, the system output is given by:

$$y(s) = \widetilde{G}p_1(s)\left\{\left[1+lm_1(s)\right] + f_2(s)\left[1+lm_2(s)\right]\right\}u_1(s). \tag{14}$$

From this expression we can identify the overall multiplicative uncertainty

$$lm(s) = lm_1(s) + f_2(s)lm_2(s). \tag{15}$$

This expression led to the following tuning procedure for the controllers parameters:

(a) Tune the controller C_1 to obtain the robust stability of:

$$1 + C_1(s)Gp_1(s) = 0, \tag{16}$$

modifying λ_1 and λ_2, for:

$$\overline{lm}(s) = \overline{lm_1}(s) + f_2(s)\overline{lm_2}(s) \tag{17}$$

where $f(s)$ is given by:

(b) check the robust stability of

$$1 + C_1(s)C_2(s)Gp_2(s) = 0, \tag{18}$$

for $\overline{lm_2}(s)$, if it require increase λ_2.

4.2. Cancellation design

As a general rule and from some of the above arguments it can be concluded that selecting the combined controller $C(s)$ as being of equal or higher order than $C_1(s)$ will always give a realizable controller C_2. Hence, any available design and adjustment procedure can be followed to completely define controllers C_1 and C for controlling Gp_1 and Gp_2, like if they were not related to each other. Then, the second controller C_2 is determined by:

$$C_2(s) = C(s)\left\{C_1(s)\right\}_+^{-1}, \tag{19}$$

where $\{\}_+$ refers to the portion of the transfer function without the integral action. There are no stability problems in this design technique because the zeros and poles of controllers C_1 and C_2 are stable and known.

4.3. Choice of κ, η and u_0

In this framework η is used to drive the steady-state value of u_1 to $u_0 \pm \kappa$ and has no effect on the steady-state of u_1, u_0 defines the steady-state value of u_1 and κ defines the region where the system output is only controlled by Gp_1. However, parameters u_0 and κ of the decision function (4) can be employed to satisfy some additional objective than control objectives.

If the objective is to *obtain a good transient behavior*, Gp_1 must be kept active in the wider possible range with a minimum intervention of Gp_2. Assuming that setpoints changes are bigger than disturbances changes, the parameters of the decision function (4) are given by:

$$u_0 = \frac{u_{1\max}+u_{1\min}}{2} - \frac{\alpha}{Kp_1}\max\left\{\mathrm{mean}\left(r(t)\right), \mathrm{mean}\left(d(t)\right)\right\} \quad |\alpha| \le 1, \tag{20a}$$

$$\eta = 0 \tag{20b}$$

$$\kappa = 0, \tag{20c}$$

where α is a defined user parameter. This selection implies the use of u_2 only when $u_1 \notin [u_{1\min}, u_{1\max}]$ to drive the steady-state of u_1 to $u_{1\max}$ or $u_{1\min}$. This is a desirable feature for the control system since it tends to keep the fastest loop working.

If the objective is to *minimize the steady-state value* u_1 employed to control the system, Gp_1 must only control the system during the transient period. Therefore, the parameters of the decision function (4) are given by:

$$u_0 = 0, \tag{21a}$$

$$\eta > 0, \tag{21b}$$

$$\kappa = 0. \tag{21c}$$

This selection implies the use of u_2 to provide the steady-state value of $y(t)$, while u_1 is only active during the transient period. Finally, if the objective is a combination of the previous ones, Gp_1 must be kept active in a range such that it can handle the most frequently changes. Therefore, the parameters of the decision function (4) are given by:

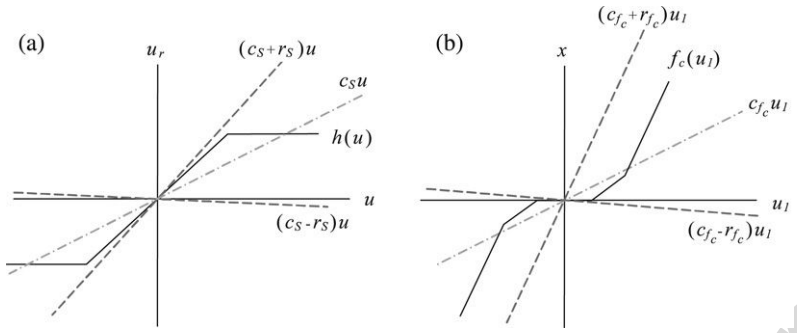

Fig. 8. Nonlinearities and approximations for stability analysis: (a) saturation and (b) decision function.

$$u_0 = \frac{u_{1\max} + u_{1\min}}{2} - \frac{\alpha}{Kp_1}\max\{\text{mean}(r(t)), \text{mean}(d(t))\} \quad |\alpha| \le 1, \tag{22a}$$

$$\eta > 0, \tag{22b}$$

$$\kappa = \frac{\beta}{Kp_1}\max\{\text{var}(d(t))\} \quad \beta \ge 0, \tag{22c}$$

where α and β defined user parameters. This selection implies the use of u_2 only when $u_1 \notin [u_0 + \kappa, u_0 - \kappa]$ to drive the steady-state of u_1 to $u_1 \pm \kappa$. This is a desirable feature for the control system since it tends to keep the fastest loop working for the most frequent changes.

To explain these concepts, let us consider the case of the heat exchangers system considered in Section 2. In this configuration the service equipment works permanently and the bypass ratio works closed such that recovered energy is maximized.

In this problem, the parameters u_0 and κ correspond to the steady-state of service energy level, which implies a loss of process efficiency, and the range of the system output that is only controlled by the service. If the objective is to obtain a good dynamic behaviour, the parameters must be set to $u_0 = 0.5, \eta = 0$ and $\kappa = 0$ respectively. In the opposite case, if the objective is maximize the amount of energy recovered, the parameters must be fixed to $u_0 = 0, \eta = 0$ and $\kappa = 0$. In this case, the split-range control is recovered. Finally, if the objective is maximize the amount of energy recovered while keeping good closed-loop performance, the parameters must be given by (22).

5. Stability analysis

A general stability analysis for the cooperative-feedback control can be performed using different frameworks: (a) a stability analysis of the resulting nonlinear system [27], (b) a stability analysis of linear systems containing time-varying parameters [28,29] or (c) a stability analysis of switched linear system [30]. In the first case the nonlinearities involved in the system – saturations and decision function – are approximated through a conic sector and then the resulting linear system is analysed using robust control tools. In the second approach, the stability of each linear system is guaranteed and then the stability of the switching between them is analysed using describing function techniques [27].

Since the nonlinearities involved in the cooperative-feedback control, the decision function and the saturations, satisfied the sector nonlinearity condition [27]

$$\left|\frac{h(u) - cu}{u}\right|^2 < r^2 - \varepsilon \qquad \forall u \ne 0, \varepsilon > 0, \tag{23}$$

the nonlinearities can be approximated by (see Fig. 8)

$$h(u) \approx (c \pm r)u,$$

where c is the gain of the linear model and r is the uncertainty of the linear model. Then, the controllers are tuned to obtain the robust stability of the closed-loop system for the overall uncertainties [25] the model and the approximation errors r. This approach leads to an over conservative tune due to the conservativeness of the process gain, introduced by the approximation (23). Therefore, the resulting closed-loop performance will be poor and the response will be sluggish.

The stability analysis of the cooperative-feedback control from the switching system point of view implies the stability analysis of every single or combined loop and the stability analysis for a general switching sequence between these loops.

In a first step, the stability of each closed-loop systems is studied. While $|\tilde{u}_1| < \kappa$ the characteristic equation for the primary control loop includes Gp_1 and C_1 only, i.e. the stability condition may be written as follows:

$$1 + Gp_1(s)C_1(s) \ne 0 \quad \forall s \in C^+, \tag{24}$$

where C^+ stands for the right-side complex plane. The second important stability condition is for the secondary loop which works through the manipulated u_2 when u_1 is saturated:

$$1 + Gp_2(s)C_2(s)C_1(s) \ne 0 \quad \forall s \in C^+. \tag{25}$$

Finally, for the intermediate case when $\eta > 0, |\tilde{u}_1| > \kappa$ and $\tilde{u}_1 \in [\tilde{u}_{1\min}, \tilde{u}_{1\max}]$, two control paths coexist simultaneously: one through u_1 and the other through u_2. Then, the condition takes the form:

$$1 + C_1(s)Gp_1(s) + \eta C_1(s)C_2(s)Gp_2(s) \ne 0 \quad \forall s \in C^+. \tag{26}$$

The first two conditions can be satisfied sequentially, (24) while adjusting controller C_1, and (25) while adjusting controller C_2. Hence, the stability problem of (26) is automatically satisfied for the nominal system. This result is summarized in the following theorem:

Theorem 1. *Given a two inputs and one output system with stable transfer function and $\eta \geq 0$, then the combined closed-loop system:*

$$1 + C_1(s)Gp_1(s) + \eta C_1(s)C_2(s)Gp_2(s) = 0$$

resulting from the application of the flexible-structure control is stable if:

$$1 + Gp_1(s)C_1(s) \neq 0 \quad \forall s \in C^+,$$
$$1 + Gp_2(s)C_2(s)C_1(s) \neq 0 \quad \forall s \in C^+.$$

Proof. Given the closed-loop equation

$$1 + C_1(s)Gp_1(s) + \eta C_1(s)C_2(s)Gp_2(s) = 0,$$

the characteristic equation of the interactive closed-loop becomes:

$$\lambda_1\lambda_2^2 s^2 + \lambda_2 (\lambda_2 + 2\eta) s + \eta = 0. \tag{27}$$

The poles of the closed-loop system p_1 and p_2 are given by:

$$p_{1,2} = -\frac{\lambda_2 + 2\eta}{2\lambda_1\lambda_2} \pm \sqrt{\frac{(\lambda_2 + 2\eta)^2 - 4\lambda_1}{4\lambda_1^2\lambda_2^2}}, \tag{28}$$

therefore it is clear that the stability of the closed-loop system only depends on the values of the parameters of the controllers (λ_1 and $\lambda_2 T_F$) and the decision function (η). Since $\lambda_1 > 0$, $\lambda_2 > 0$ and $\eta > 0$, the closed-loop system will be stable for any value of λ_1, λ_2 and η. □

Remark 3. This result can be easily extended to uncertain systems just considering the worst case plants:

$$\overline{Gp_i}(s) = \widetilde{Gp_i}(s)\left[1 + \overline{lm_i}(s)\right] \quad i = 1, 2$$

in the previous theorem. This fact implies the closed-loop poles of the real systems $Gp_i(s) i = 1, 2$ are confined to a region defined by the models $\widetilde{Gp_i}$ and uncertainties $\overline{lm_i}$.

To end this analysis, some comments about the effect of the parameters variations on the poles location of the cooperative control are given. If $\eta = 0$ and $\lambda_1 < \lambda_2$ the closed-loop poles will be located at $p_1 = 0$ and $p_2 = -\lambda_1^{-1}$. For any increment of η and λ_2 or a decrement of λ_1, p_1 will remain fix at the origin but p_2 will move to the left. While $\lambda_2 + 2\eta \gg \lambda_1$ the closed-loop poles will be located at:

$$p_1 = 0, \qquad p_2 = -\frac{\lambda_2 + 2\eta}{\lambda_1\lambda_2}. \tag{29}$$

Since $\lambda_1 < \lambda_2$, the closed-loop poles will be real and the overshoot in the closed-loop response will be produced by switching in the system. In the case of the cooperative control, the property of independent selection of the natural frequency and the damping ratio of the closed-loop system is losing because they are function of λ_1, λ_2 and η.

Finally, the stability analysis of the switching sequence implies the analysis of the following systems:

$$1 + C_1(s)Gp_1(s) + S(s)\eta C(s)Gp_2(s) = 0, \tag{30a}$$

$$1 + S(s)C_1(s)Gp_1(s) + C(s)Gp_2(s) + S(s)(\eta - 1)C(s)Gp_2(s) = 0, \tag{30b}$$

$$1 + S(s)C_1(s)Gp_1(s) + [1 - S(s)]C(s)Gp_2(s) = 0, \tag{30c}$$

that represent all possible changes in the system. In these expressions $S(s)$ is the Fourier transform of the switching function $S(t)$ given by:

$$S(t) = \frac{1}{2}[1 - g(t)], \tag{31}$$

where $g(t)$ is a scalar signal that only assumes the value -1 or $+1$.

The Eq. (30a) represents the changes in the system when the secondary loop becomes active at the same time as the primary loop ($\tilde{u}_1 \in [\kappa, \tilde{u}_{1\max}]$). The second equation, Eq. (30b), represents the change in the system when $\tilde{u}_1$ is saturated ($\tilde{u}_1 \notin [\tilde{u}_{1\max}, \tilde{u}_{1\min}]$), then only the second loop controls the system output. Finally, the Eq. (30c) represents the direct transition from $|\tilde{u}_1| < \kappa$ to $\tilde{u}_1 \notin [\tilde{u}_{1\max}, \tilde{u}_{1\min}]$, this fact means that the main loop becomes inactive at the same time that the secondary loop is activated.

For switching sequences slower than the system dynamic, the stability of the overall closed-loop system is guaranteed [30]. The stability of an arbitrary switching sequence between these systems can be analysed using describing function techniques and harmonic balance explained by Leith et al. [30]. Firstly, the nonlinearities are approximate through a Fourier series:

$$S(t) = f_0 + f_1 \cos(\omega t + \phi) + h.o.t,$$

then, due to the low-pass characteristic of the system $S(t)$ may be approximate

$$S(t) \approx f_0 + f_1 \cos(\omega t + \phi).$$

For the controllers resulting from the IMC design, the transfer function of the equivalent linear system of (30) is given by:

$$H_1(s) = -\frac{\eta f_1 (2\lambda_1 s + 1)}{\lambda_1\lambda_2^2 s^2 + \lambda_2 (\lambda_2 + 2\eta) s + \eta f_0}, \tag{32a}$$

$$H_2(s) = -\frac{f_1[\lambda_2 s + (\lambda_2 - \lambda_1)]}{\lambda_1\lambda_2^2 s^2 + \lambda_2[f_0 + 2\lambda_1(1 + (\eta - 1)f_0)]s + \lambda_1(1 + (\eta - 1)f_0)}, \tag{32b}$$

$$H_3(s) = -\frac{f_1[\lambda_2 s + (\lambda_2 - \lambda_1)]}{\lambda_1\lambda_2^2 s^2 + \lambda_2[(\lambda_2 - 2\lambda_1)f_0 + 2\lambda_1]s + (1 - f_0)\lambda_1}. \tag{32c}$$

Finally, the resulting transfer functions are analysed using the method of harmonic balance to determine the stability of the switching sequence. This method predicts instability everywhere the magnitude of the Bode plot of the resulting linear system exceeds unity.

6. Simulation and results

In this section a simulation example of a linear model and the heat exchanger system showed in Fig. 2 are considered to analyse and evaluate the effectiveness of the cooperative-feedback control structure. The linear model was previously

used by other authors [8,21] to evaluate cooperative control schemes. The heat exchanger system was previously analysed by several authors [9,15,16,31].

Example 1. In this example the cooperative-feedback control structure is analysed and evaluated for setpoint tracking and disturbance rejection. The effect of the parameters of the decision function on the closed-loop response are showing. The linear system previously used by Wang et al. [8] is considered, the transfer functions are given by:

$$Gp_1(s) = \frac{e^{-4s}}{(2s+1)^2} \cong \frac{e^{-5s}}{2.75s+1}, \tag{33}$$

$$Gp_2(s) = \frac{2e^{-10s}}{(6s+1)(17s+1)}. \tag{34}$$

The manipulated variables, u_1 and u_2 are constrained to $u_i \in [-1,+1]\, i = 1,2$. The controllers were developed using a Smith predictor structure to compensate the time delays of the process and improve the closed-loop performance. Firstly, the controller C_1 was designed using the formulas (9) and obtain a response without offset. This means that controller C_1 is a PI controller, whose parameters are:

$$K_{C_1} = \frac{5.5}{\lambda_1}, \tag{35a}$$

$$T_{I_1} = 2.75. \tag{35b}$$

To design the controller C_2, the transfer function Gp_2 was approximated using (10), the result was:

$$Gp_2(s) \simeq \frac{2e^{-10s}}{(2.75s+1)(18.75s+1)}. \tag{36}$$

Then, the controller C_2 was designed to track a ramp setpoint using Gp_2. This means that the controller C_2 is a PID controller, whose parameters are given by (21):

$$K_{C_2} = \lambda_1 \frac{2\lambda_2 + 18.75}{\lambda_2^2}, \tag{37a}$$

$$T_{I_2} = 2\lambda_2 + 18.75, \tag{37b}$$

$$T_{D_2} = 37.5 \frac{\lambda_2}{2\lambda_2 + 18.75}. \tag{37c}$$

Since there is no uncertainty, the parameters λ_1 and λ_2 were determined through simulations to obtain the best possible performance. The value of these parameters is:

$$\lambda_1 = 1.75, \qquad \lambda_2 = 10.5. \tag{38}$$

An IMC antiwindup scheme is included in controller C to compensate the effect of the constraint in u_2. The parameters of the decision function (4) were chosen to obtain a good performance and minimize the use of u_1, using the formulas (22), the result is:

$$u_0 = 0, \qquad \kappa = 0.25, \qquad \eta = 0. \tag{39}$$

Finally, the stability of the system for the switches is analysed. Fig. 9 shows the Bode plots for the transfer functions (32) for parameters (38) and (39). It is easy to see the resulting linear system does not exceed unity, therefore all possible switching between these systems is stable.

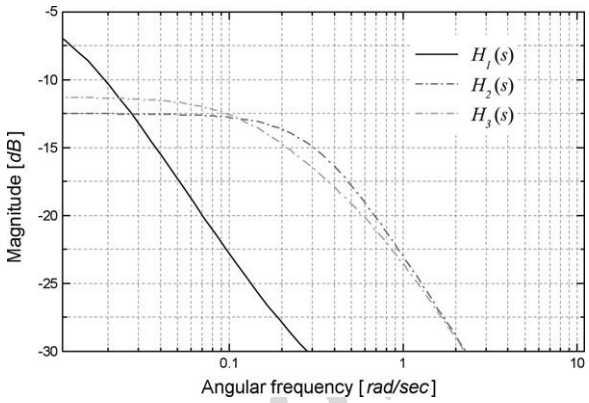

Fig. 9. Bode plots associated with approximated analysis of transfer functions (26).

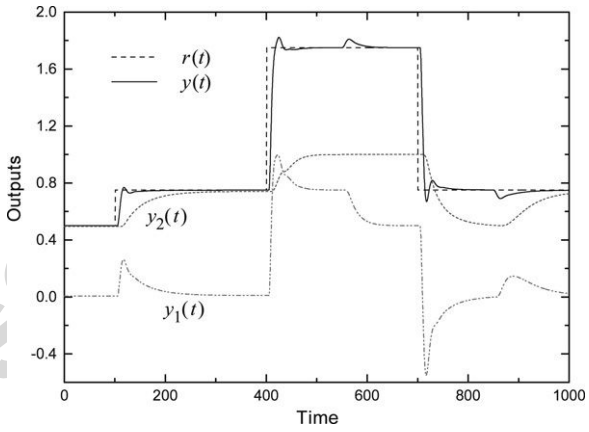

Fig. 10. Transient responses of the system output (y) and individual outputs (y_1 and y_2) to a sequence of setpoint and load changes.

In order to evaluate the performance of the proposed control scheme, a sequence of reference and load disturbance changes were introduced. The setpoint r was changed in intervals of 300 s from 0.5 to 0.75, then it steps to 1.5 and finally the setpoint returns to 0.75. A load disturbance of 0.5 is introduced in the system 550 and the retired at 850.

In Fig. 10 the responses of the system outputs obtained by the cooperative-feedback control scheme can be seen. This figure shows how both individual outputs, y_1 and y_2, are combined to produce a better performance and u_1 is kept as small as possible. The excellent performance is obtained because the fastest loop is kept working in the entire operating range and the proposed control scheme takes in account the dynamic of the auxiliary manipulated variable. We can also see how the proposed control scheme extend the operating range of the system, solving the controllability problem, by combining both manipulated variables. In Fig. 11 the behaviour of the manipulated variables (u_1 and u_2) and the auxiliary signal (x) obtained by the cooperative-feedback control scheme for the given setpoint and load changes can be evaluated. It is clear that the interaction between both loops improves the performance of the closed-loop performance, specially when the control needs to be transferred from u_2 to u_1.

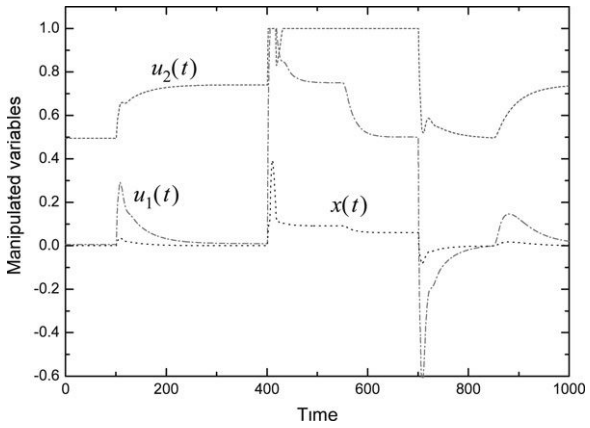

Fig. 11. Transient responses of manipulated variables (u_1 and u_2) and auxiliary signal (x) to a sequence of setpoint and load changes.

To address the effects of the protection level η the proposed algorithm is simulated with different values of it. The results with different η are shown in the Figs. 12 and 13. It can be seen that the higher the level of η the better the performance, since both transfer functions control the system output. The system output is the result of the combination of both systems (see Fig. 12), the transient is controlled by Gp_1 while the steady-state is provided by Gp_2. The effect of varying η is to increase the interaction between both control loops. Fig. 13 shows the control actions associated with the responses of Fig. 12. In this figure the modification of the closed loop behaviour can be seen: the manipulated variables go from overdamped to underdamped when η is increased.

Example 2. This example shows some results obtained applying the cooperative-feedback control to the heat-exchanger system of Fig. 2. In this configuration the main objective of the heat-exchanger I_1 is to preserve the controllability of the system in the entire operational range, specially under disturbances, while the main control task is provided by the service S. This control configuration is preferred when a wide operational region is needed, which means that the service equipment S works along important periods of time to control the final temperature T_{h_1}, however operative changes or unexpected load disturbances might saturate it. The exchanger I_1 is used to extend the operational region by modifying the amount of energy recovered.

The flowrate and temperature of streams C_1 and H_1 were modelled by a stochastic stationary signals described by their mean value plus a coloured noise disturbance, which was modelled as white noise filtered by a first order filter whose bandwidth is narrower than the system bandwidth. The value of the parameters of the streams (density (ρ), specific heat (C_p), mass flow rate (w), inlet and outlet temperatures (T^{in} and T^{out})) and heat exchangers are given in Tables 1 and 2. The parameters of the heat exchangers are: heat exchanger area (A_t), global heat transfer coefficient (U), holdup volume on the tube side (V_{tt}), holdup volume on the shell side (V_{tc}), number of vertical baffles (N_b) and number of tube passes (M). All these design parameters are required by the nonlinear model developed by Correa and Marchetti [32], which was used in this work to obtain the simulation results. Data are given in international units.

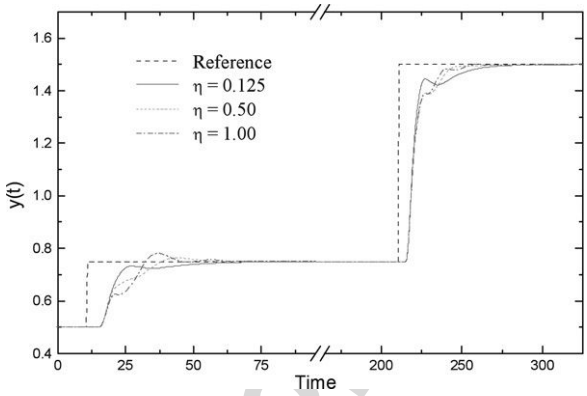

Fig. 12. Setpoint responses obtained for different values of η.

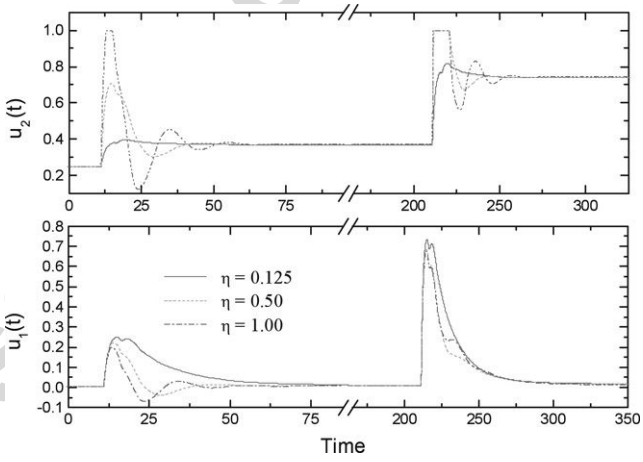

Fig. 13. Primary and auxiliary variables corresponding to setpoint changes of Fig. 12.

Table 1
Stream parameters

Stream	ρ	C_p	w	T^{in}	T^{out}
C_1	1000	4.179	9.57 ± 2.0	65 ± 5.0	–
H_1	1000	4.184	4.78 ± 1.0	130 ± 2.0	100
S	1000	4.179	7.18	30	–

Table 2
Heat-exchanger parameters

A_t	U	V_{tt}	V_{tc}	N_b	M
20	1	0.07	0.15	9	1

Fig. 14 shows the open-loop response of the system for changes in the service (u_1) and bypass flowrate (u_2). In these figures we can see that the dynamic of the system is similar for different values of the manipulated variables, only differ in the steady-state gain. Therefore, for design purpose, only uncertainty in the steady-state gain was assumed. Six linear models for each manipulated variable were determined from the output temperature responses shown in Fig. 14, using a

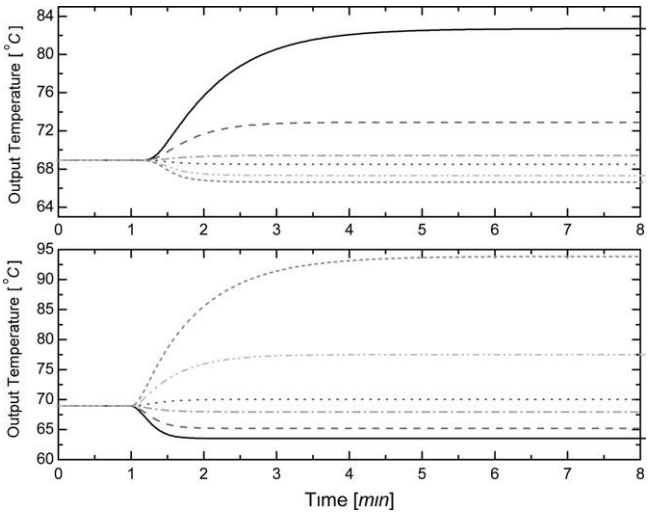

Fig. 14. Open-loop behaviour of the heat exchanger system to step changes in (a) bypass and (b) service flowrates.

subspace identification algorithm.

$$Gp_1(s) = \frac{T_{h_1}(s)}{u_1(s)} = Kp_{1i}\frac{e^{-5.5s}}{15.5s+1}, \tag{40a}$$

$$Gp_2(s) = \frac{T_{h_1}(s)}{u_2(s)} = Kp_{2i}\frac{e^{-25.3s}}{36.5s+1}. \tag{40b}$$

Table 3 shows the gains of each transfer function that define the polytopic linear model associated to the nonlinear behaviour of the heat-exchanger system in the entire operating domain.

The manipulated variables of the service and bypass flowrate, u_1 and u_2, are constrained to $u_i \in [0, 1]\, i = 1, 2$. The controllers were developed using a Smith predictor structure to compensate the time delays of the process and improve the closed-loop performance. Firstly, the controller C_1 is designed using the formulas (9) and obtain a response without offset. This means that the controller C_1 is a PI controller, whose parameters are:

$$K_{C_1} = \frac{15.5}{\tilde{K}p_1\lambda_1}, \tag{41a}$$

$$T_{I_1} = 15.5. \tag{41b}$$

To tune the controller C_2, we approximate Gp_2 using (10), the result is:

$$Gp_2(s) \simeq \tilde{K}p_2\frac{e^{-18.9s}}{(15.5s+1)(29.7s+1)}. \tag{42}$$

Then, the controller C_2 was designed to track a ramp setpoint using Gp_2. This means that the controller C_2 is a PID controller, whose parameters are given by: (21)

$$K_{C_2} = \frac{\tilde{K}p_1}{\tilde{K}p_2}\lambda_1\frac{2\lambda_2+29.7}{\lambda_2^2}, \tag{43a}$$

$$T_{I_2} = 2\lambda_2 + \tau_{p2} = 2\lambda_2 + 29.7, \tag{43b}$$

$$T_{D_2} = \frac{2\lambda_2\tau_{p2}}{2\lambda_2+\tau_{p2}} = 29.7\frac{\lambda_2}{2\lambda_2+29.7}. \tag{43c}$$

Table 3
Gains of polytopic linear models

Δu	Kp_{1i}	Kp_{2i}
+0.40	−13.52	+34.45
+0.20	−18.61	+19.91
+0.05	−19.41	+10.01
−0.05	−22.83	+8.41
+0.20	−42.92	+7.92
−0.40	−62.37	+5.71

The parameters λ_1 and λ_2 are determined through simulations to obtain the best possible performance for the worst case model (the highest gains: $\tilde{K}p_1 = -62.37$ and $\tilde{K}p_2 = 34.45$), the value of these parameters is:

$$\lambda_1 = 2.75, \qquad \lambda_2 = 12.5. \tag{44}$$

An IMC antiwindup scheme is included in controller C to compensate the effect of the constraint in u_2. Finally, the parameters of the decision function (4) were chosen to obtain a good performance and minimize the use of u_1. The parameters of the decision function were determined using the formulas (22), the result is:

$$u_0 = 0.1, \qquad \kappa = 0, \qquad \eta = 0.5. \tag{45}$$

Finally, the stability of the system for the switches is analysed using the harmonic balance technique for all linear models of the polytopic representation, the resulting linear systems are stable for all possible switching between these systems are stables.

In this example the cooperative-feedback control is compared with the flexible-structure control [21]. The controller C_1 is designed using the IMC tuning formula and obtain a response without offset. This means that the controller C_1 is a PI controller, whose parameters are:

$$K_{C_1} = -0.3706, \qquad T_{I_1} = 23.67.$$

The controller C_2, which manipulates the bypass ration of I_1, is designed through the cancellation approach

$$C_2(s) = C_1^{-1}(s)C(s),$$

once the parameters of the combined controller C are determined. In this application, a PID controller is adopted for controller:

$$C(s) = K_C\left(1 + T_D s + \frac{1}{T_I s}\right).$$

Hence, the controller C_2 results a PD controller:

$$C_2(s) = \frac{K_C T_{I_1}}{K_{C_1} T_{I_1}}\frac{(T_I + T_D)\, s + 1}{T_{I_1} s + 1} = K_{C_2}\frac{bs+1}{as+1}$$

which is activated just to avoid bypass saturation. Now, we tune the controller C employing Ziegler–Nichols procedure. The parameter values obtained for controller C_2 are:

$$K_{C_2} = 0.245, \qquad a = 23.67, \qquad b = 27.5.$$

In Fig. 15 it is possible to see the responses obtained by the two control schemes. A better the performance for the overall

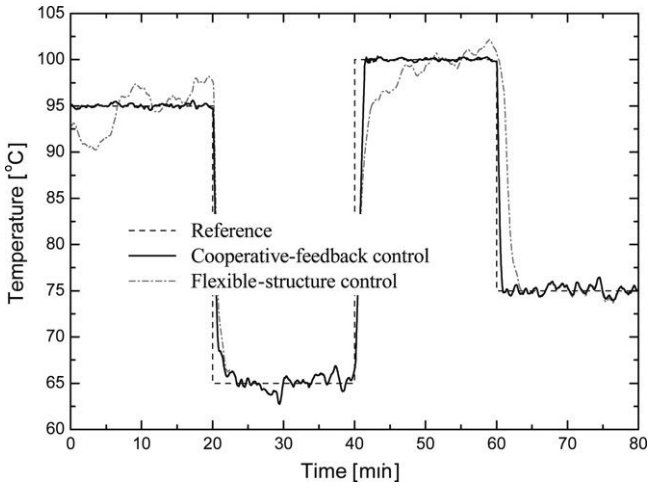

Fig. 15. Transient responses of the system output T_{h_1} to a sequence of setpoint changes and load disturbances.

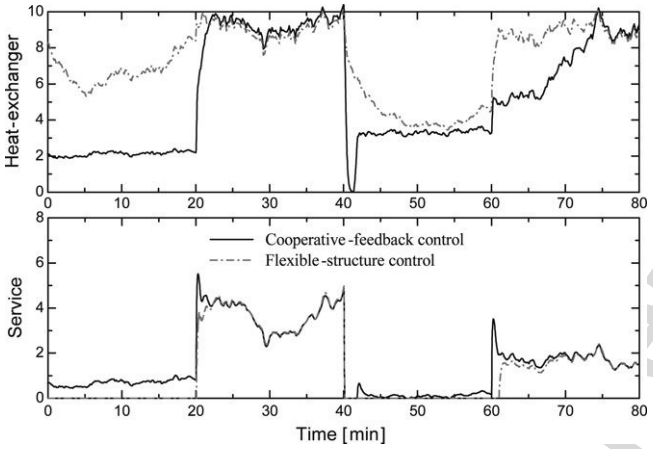

Fig. 16. Transient responses of the bypass and service flowrates corresponding to Fig. 15.

response is obtained by the cooperative feedback control in spite that both control schemes used the same amount of service s. This happen because the heat exchanger I_1 is in charge of the regulation of T_{h_1} in the case of flexible-structure control, which leads to a poor performance due to the dynamic characteristics of the heat exchanger. In the case of the cooperative feedback, is the service S who is in charge of the regulation, and therefore the better performance. It is interesting to observe that both control schemes have similar performance for the second change. In this case both control schemes employed the S to control T_{h_1}.

Fig. 16 shows the bypass and service responses corresponding to the setpoint changes. They show how the service flow rate of the cooperative-feedback control scheme avoids the saturation and takes control of the operation. It is interesting to see that in the case of the first and third setpoint changes, the service flowrate of both control schemes are similar. They only differ in the transient behaviour to achieve the steady-state values: the cooperative-feedback is faster and avoids the kick-off effect due to its habituating nature. On the other hand, the cooperative-feedback sacrifices energy integration in order to obtain a superior performance in the initial time.

7. Conclusions

A new control structure is proposed for dealing with constraints on manipulated variables process shows at least two input variables associated to the control target. Cooperative-feedback control refers to the resulting control system, which employs both manipulated variables to control the systems and is able to coordinate and switch from one closed-loop to another in order to keep system controllable. This habituating characteristic of the control system is particularly useful when the optimal operating point locates near to a limit constraint of the main manipulated variable. Issues related to design and tuning a cooperative-feedback control system are discussed. The application to a linear and a nonlinear system shows the trade off between process efficiency and controllability.

Acknowledgments

The author is grateful for the financial support for this work provided by the Engineering and Physical Science Research Council (EPSRC) grant Industrial Non-linear Control and Applications GR/R04683/01. Thanks are due to Dr Hao Xia for valuable discussions for the suggestions to improve the paper.

References

[1] Hanus R, Kinnaert M, Henrote J. Conditioning techniques, a general anti-windup and bumpless transfer method. Automatica 1987;23:729–39.
[2] Peng Y, Vrančić D, Hanus R, Weller S. Anti-windup designs for multivariable controllers. Automatica 1998;33(12):1559–65.
[3] Kothare M, Campo P, Morari M, Nett C. A unified framework for the study of anti-windup design. Automatica 1994;30:1869–83.
[4] Krikelis N, Barks S. Design of tracking systems subject to actuator saturation and integrator windup. International Journal of Control 1984; 39:667–82.
[5] Glattfelder A, Schaufelberger W. Control systems with input and output constraints. In: Advanced textbooks in control and signal processing series. Springer Verlag; 2003.
[6] Saberi A, Stoorvogel A, Sannuti P. Control of linear systems with regulation and input constraints. Springer Verlag; 1999.
[7] Chen C, Peng S. Learning control of process systems with hard constraints. Journal of Processing Control 1999;9:151–60.
[8] Wang Q, Zhang Y, Cai W, Bi Q, Hang C. Cooperative control of multi-input single-output processes: On-line strategy for releasing input saturation. Control Engineering Practice 2001;9:491–500.
[9] Stephanopoulos G. Chemical process control: An introduction to theory and practice. Englewood Cliffs (NJ): Prentice-Hall; 1984.
[10] Shinskey F. Process control systems: Application, design and tuning. 3rd ed. New York: McGraw-Hill; 1988.
[11] Gao Z. Stability of the pseudo-inverse method for reconfigurable control system. International Journal of Control 1991;8:469–74.
[12] Aguilera N, Marchetti J. Optimizing and controlling the operation of heat exchanger networks. AIChE Journal 1998;44:1090–104.
[13] Marselle D, Morari M, Rudd D. Design of resilient processing plants: II design and control of energy management system. Chemical Engineering Science 1982;37:259–70.
[14] Mathisen K. Integrated design and control of heat exchanger networks. Ph.D. thesis. Trondheim (Norway): Univ. of Trondheim; 1994.
[15] Luyben W. Process modelling, simulation and control for chemical engineers. New York: McGraw-Hill; 1990.

[16] Shinskey F. Process control systems: Application, design and tuning. New York: McGraw-Hill; 1988.
[17] Popiel L, Matsko T, Brosilow C. Coordinated control. In: Morari M, McAvoy T, editors. Chemical process III. New York: Elsevier; 1986. p. 295–315.
[18] Chia T, Brosilow C. Modular multivariable control of a fractionator. Hydrocarbon Processing 1991;61.
[19] Balchem J, Mumme K. Process control: Structures and applications. New York: Van Nostrand Reinhold; 1988.
[20] Willians S, Hrovat D, Davey C, Maclay D, van Crevel J, Chen L. Idle speed control design using an H_∞ approach. In: Proc. American control conf. 1992. p. 1950–5.
[21] Giovanini L. Flexible-structure control. ISA Transactions Journal 2004; 43(3):361–76.
[22] Lurie B, Enright P. Classical feedback control with Matlab. New York: Marcel Dekker; 2000.
[23] Henson M, Ogunnaike B, Schwaber J. Habituating control strategies for process control. AIChE Journal 1995;41(3):604–18.
[24] Smith O. Close control of loops with dead time. Chemical Engineering Progress 1957;53:217–9.
[25] Morari M, Zafiriou E. Robust process control. Englewood Cliffs: Prentice-Hall; 1989.
[26] Chien I, Fruehauf P. Consider IMC tuning to improve controller performance. Chemical Engineering Progress 1990;86:33–41.
[27] Khalil K. Nonlinear system analysis. New York: Macmillan; 1992.
[28] Gahinet P, Apkarian P, Chilali M. Parameter-dependent Lyapunov functions for real parametric uncertainty. IEEE Transactions on Automatic Control 1995;39(7):1095–108.
[29] Tetsuya I, Shibata G. LPV system analysis via quadratic separator for uncertain implicit systems. IEEE Transactions on Automatic Control 2001;46(8):1195–208.
[30] Leith D, Shorten R, Leithead W, Mason O, Curran P. Issues in the design of switched linear control systems: A benchmark study. Interantional Journal of Adaptive Control and Signal Processing 2003;17: 103–18.
[31] Rotea M, Marchetti J. Integral control of heat-exchanger-plus-bypass systems. In: IEEE international conf. on control applications. 1997. p. 151–6.
[32] Correa D, Marchetti J. Dynamic simulation of shell-and-tube heat exchangers. Heat Transfer Engineering 1987;8:50–9.

Leonardo Giovanini received the B.Sc. (Honours) degree in Electronic Engineering from the Universidad Tecnolgica Nacional (Argentina) in 1995, and the Ph.D. degree in Engineering Science from Universidad Nacional del Litoral (Argentina) in 2000. From 1998 until 2001 he was lecturer in the Department of Electronic Engineering at Universidad Tecnogica Nacional (Argentina). Since 2002, he has been working as Senior Research Fellow in the Industrial Control Centre, University of Strathclyde. Since 2005, he is the Centre0 Technical Manager and member of the Institute of Engineering and Technology. He has published more than forty technical papers. His research interests include predictive control for non-linear systems, robust adaptive control, fault detection and isolation and control of complex systems.